Morphology and Development of a New Species of Balanoglossus (Hemichordata: Enteropneusta: Ptychoderidae) from Shimoda, Japan

Authors: Miyamoto, Norio, and Saito, Yasunori

Source: Zoological Science, 24(12) : 1278-1285

Published By: Zoological Society of Japan

URL: https://doi.org/10.2108/zsj.24.1278

ZOOLOGICAL SCIENCE **24**: 1278–1285 (2007)

Morphology and Development of a New Species of *Balanoglossus* (Hemichordata: Enteropneusta: Ptychoderidae) from Shimoda, Japan

Norio Miyamoto and Yasunori Saito*

Shimoda Marine Research Center, University of Tsukuba, Shimoda, Shizuoka 415-0025, Japan

The morphology and development of a new species of the genus *Balanoglossus* belonging to the family Ptychoderidae are described in detail. This acorn worm was collected from the sandy seashore in the cove near Shimoda Marine Research Center, University of Tsukuba (Shimoda, Shizuoka Prefecture, Japan). This acorn worm is easily distinguished from other balanoglossids by a characteristic hepatic region. There are two kinds of hepatic saccules: large, dark-colored saccules in the anterior region and small, light-colored saccules in the posterior region. Between the two subregions of the hepatic region, there is a small region that has no or tiny saccules. This species does not form distinct burrows or mounds of casts. The breeding season is in winter. The process of embryogenesis from fertilization to metamorphosis was observed. A shift in seawater temperature from about 13°C to about 9°C induced gamete release. Two days after fertilization, embryos hatched and became typical feeding tornaria larvae. Two months after fertilization these larvae metamorphosed into juveniles and began their benthic life.

Key words: Hemichordata, acorn worm, *Balanoglossus*, new species, morphology, development

INTRODUCTION

Enteropneusts are free-living, vermiform marine invertebrates mostly living in the sediment and are classified into approximately 80 species. The class Enteropneusta is composed of five extant families: Ptychoderidae, including the genus *Balanoglossus*; Harrimaniidae; Spengelidae; Saxipendiidae from hydrothermal vents (Woodwick and Sensenbaugh, 1985); and Torquaratoridae from the deep sea (Holland *et al.,* 2005). Ptychoderids are the most morphologically complex of the Enteropneusta. They have genital ridges, hepatic saccules, synapticles in the gill bars, peribuccal space, parabranchial ridge, lateral septa, dorsolateral ciliated groove, and pygochord, but they do not have the vermiform process of the stomochord and esophageal pores (Benito and Pardos, 1997). About 30 species have been described from this family. The family Ptychoderidae is composed of three genera: *Balanoglossus*, *Glossobalanus*, and *Ptychodera*. Members of the genus *Balanoglossus* have well-developed genital wings, small gill pores, and lateral septa that connect to genital wings at the dorsal side where primary gonad pores open. About 17 species have been described in the world (Horst, 1939, 1940); until now, only two species, *Balanoglossus carnosus* and *Balanoglossus misakiensis* were reported from Japan (Nishikawa, 1977).

Two types of embryonic development are known in enteropneusts. One type is direct development, and the other is indirect development with a planktonic larval stage called a tornaria. Species of the family Ptychoderidae usually have the planktonic larval stage in their life cycle. However, the development of hemichordates has not been investigated extensively, because it is difficult to collect adult worms, to obtain mature gametes, and to keep larvae in the laboratory. Only one hemichordate, *Balanoglossus misakiensis*, with indirect development has been observed from fertilization to adult by artificial induction of gamete release under laboratory conditions (Urata and Yamaguchi, 2004). On the other hand, many tornaria larvae have been described from all over the world (Stiasny-Wijnhoff and Stiasny, 1927), including Japan (Stiasny, 1929; Tokioka, 1937), but the corresponding adult worms are still unknown for most of these species. Several stages of tornaria larvae have been described. The morphology of each, especially the Krohn stage, is different among species.

We found an undescribed acorn worm in Kujuppama, Shimoda, Japan, and induced release of its gametes in the laboratory. In the present study, we observed the morphology and development of this acorn worm, which belongs to the genus *Balanoglossus*. We compared features of this species with those of other known balanoglossid acorn worms and tornaria larvae.

MATERIALS AND METHODS

Balanoglossids were collected throughout the year from bouldery sand in the lower intertidal and upper subtidal zones (0–2 m in depth) at Kujuppama (34°40'4"N, 138°58'39"E), Shimoda, Shizuoka, Japan. Worms were transported to the Shimoda Marine Research Center and kept in an aquarium containing sand from Kujuppama in fresh running seawater. For histology, some worms

* Corresponding author. Phone: +81-558-22-6776;
Fax : +81-558-22-0346;
E-mail: saito@kurofune.shimoda.tsukuba.ac.jp
doi:10.2108/zsj.24.1278

were kept without sand to allow them to evacuate their gut contents. The cleaned worms were relaxed in L-menthol in filtered seawater (FSW) for about 1 hr, and then fixed in Bouin's fixative. The fixed worms were dehydrated in a graded ethanol-*n*-butanol series and embedded in paraplast (Sigma, USA). These specimens were sectioned at 7 μm, stained with Delafield's hematoxylin and eosin Y, and observed under a light microscope.

Mature worms were collected between January and March 2006 at Kujuppama. In the laboratory, they were induced to spawn gametes by shifting the seawater temperature from 13°C to 8–10°C, and fertilization was performed artificially. Embryos were cultured in FSW at 17–20°C in glass beakers. Hatched larvae were transferred to 3-L glass beakers of FSW with gentle stirring at a concentration of 100 larvae/L. The FSW in the beakers was changed every few days; after each change the larvae were fed *Chaetoceros calcitrans* (Nisshin Marine Tech Co., Yokohama, Japan) cells at a concentration of 3,000 cells/ml. Early-stage embryos and larvae were observed and photographed under a light microscope.

RESULTS

Balanoglossus simodensis n. sp.

Type series. HOLOTYPE: mature female, complete series of transverse sections, 7 μm, 66 slides (NSMT-Hem1), 22 February 2006. PARATYPES: two mature females, complete series of transverse sections, 7 μm, 61 slides (NSMT-Hem2) and 66 slides (NSMT-Hem3), 22 February 2006; mature male, (NSMT-Hem4), 22 February 2006; mature male, (NSMT Hem5), 7 December 2006; mature female (NSMT-Hem6), 7 December 2006; two mature males, (NUM-Az0626), 20 October 2006; two mature females, (NUM-Az0627), 10 January 2007. Each type specimen was collected from Kujuppama by N. Miyamoto.

Type locality. Kujuppama, Shimoda, Shizuoka, Japan.

Etymology. The species name *simodensis* refers to the type locality.

Description

Balanoglossus simodensis (Fig. 1A) is an infaunal worm living in the bouldery, sandy seashore in the inner part of the bay, where rocks provide protection against waves. This species does not build any distinct burrow nor mounds of casts. The body length is up to 10 cm when relaxed. The trunk is composed of four regions: branchiogenital, genital, hepatic, and caudal. The body length of the holotype is 7.3 cm when relaxed. The length of the each body part is as follows: proboscis, 3 mm; collar, 3.3 mm; branchiogenital region, 7 mm; genital region, 15 mm; hepatic region, about 19 mm; and caudal region, about 26 mm. However, the ratio of the length of each body region to the total length of the worm varies, because portions of individuals seem to break off and regenerate repeatedly in the wild.

The proboscis is conical, approximately the same length as the collar, and protrudes almost completely from the collar. There is no middorsal groove on the proboscis. The length and width of the collar are nearly identical. The genital wings fuse with the posterior rim of the collar; they are already so broad that their free edges touch each other at the anterior end. They reach their maximum width near the hind end of the branchial region (Fig. 1A). Because the branchial basket of this species protrudes dorsally from the dorsal epidermis, the posterior end of the branchial basket

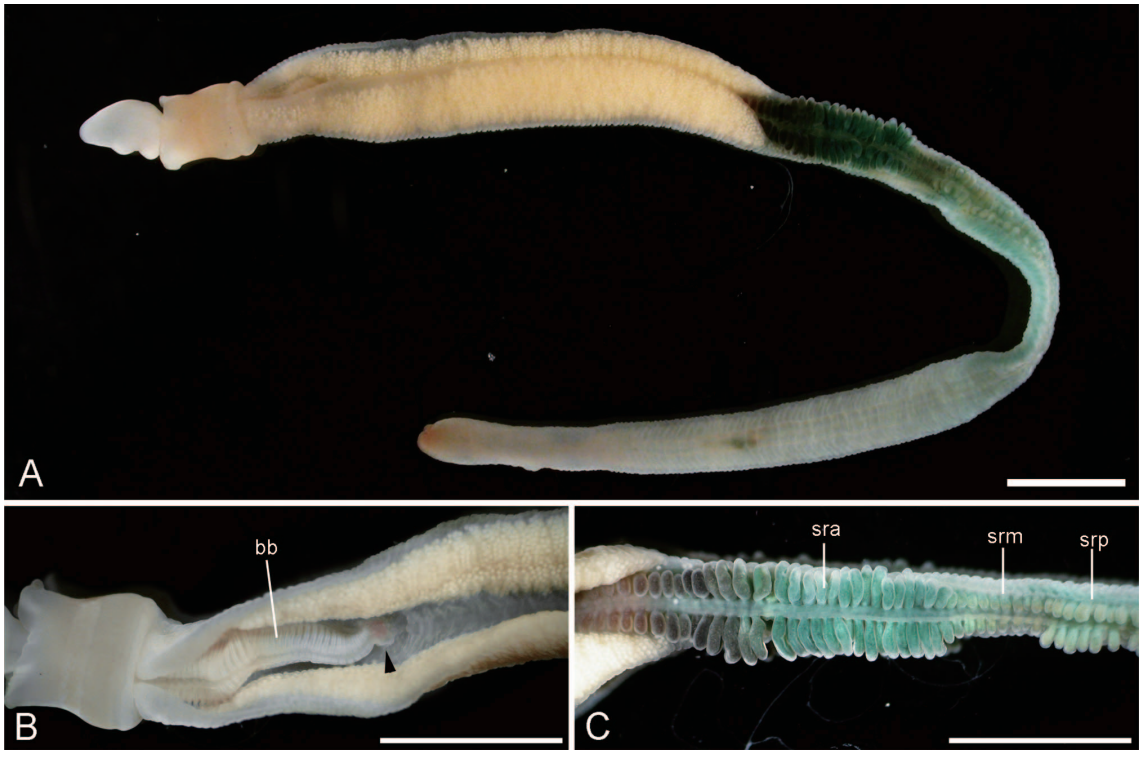

Fig. 1. Photographs of *Balanoglossus simodensis* (holotype) in the anesthetized condition. **(A)** Dorsolateral view. **(B)** Dorsal view of the collar and branchiogenital region. **(C)** Dorsal view of the hepatic region. **bb**, branchial basket; **sra**, anterior subregion of the hepatic region; **srm**, middle subregion of the hepatic region; **srp**, posterior subregion of the hepatic region. Scale bars=5 mm.

is distinct (Fig. 1B arrowhead). The hepatic saccules form a regular row on each side (Fig. 1C). There are two color variations —green and brown— of the hepatic region, which are determined by the individual worm's habitat. The most obvious external character of *B. simodensis* is the appearance of the hepatic region, which can be divided into three subregions. In the anterior subregion (Figs. 1C, 2H), there are dark-colored saccules. The anterior part of this subregion, where there are genital wings on both sides of the body, is a transitional zone that has small saccules that gradually increase in size. Where the genital wings end, the saccules abruptly increase in size and maintain this size posteriorly. In the posterior subregion of the hepatic region (Figs. 1C, 2H), there are small, light-colored saccules that gradually become smaller in size and lighter in color and finally fade out. Therefore, it is hard to determine the posterior extent of the hepatic region. Between these two subregions, there is a small, middle subregion (Figs. 1C, 2H) that has no or tiny saccules. The hepatic region is followed by the caudal region, which is so transparent that the gut contents are visible from the exterior. The anus opens at the terminus of the body. Brown pigments are deposited around the anus.

Proboscis. The thickness of the nerve tissue layer of the ectoderm of the proboscis is equal to or thicker than that of the underlying circular muscle layer, and in the posterior part of the proboscis the nerve tissue layer becomes much thicker. The longitudinal muscle fibers, as seen in a cross section of the proboscis, are well developed and are arranged in radiating plates in the anterior part of the proboscis. The dorsoventral muscle plate is poorly developed. The proboscis organs connect with the dorsal epidermis via the pericardium (Fig. 2A). The ventral septum of the proboscis extends from where the pericardium connects with the dorsal epidermis to the end of the coelomic blind sac (Fig. 2A, B). The proboscis coelom is the outside of the proboscis organs (Fig. 2A, G). Anterior to the proboscis organs, connective tissue fills the proboscis coelom (Fig. 2G). In most specimens examined, the left dorsal coelom opens to the outside of the body through the proboscis pore; however, in paratype NSMT-Hem3, the right dorsal coelom opens to the outside. The central lumen is discontinuous for the entire anterior fourth of the stomochord, whereas the central lumen is distinct in the posterior part of the stomochord. The glomerulus covers the front end and lateral sides of the pericardium and stomochord (Fig. 2A, G). There is a small dorsal glomerulus, and no glomerulus ventral to the stomochord. The U-shaped endplate (Fig. 2B), which, in cross section, encircles the ventral part of the stomochord, becomes O-shaped and smaller posteriorly in a funnel-like manner (Fig. 2C). At the apex of the funnel, the endplate connects with the body and keel of the skeleton. In some specimens (paratype NSMT-Hem2 and a specimen not included in type series), the body and keel separate just behind the beginning of the body and keel of the skeleton, but connect again in the posterior part of the body of the skeleton. The keel of the skeleton is well developed and projects into the buccal cavity (Fig. 2D). The size of the keel increases gradually; then, in the posterior half of the keel, the size gradually decreases until the keel disappears just in front of where the body of the skeleton bifurcates into two crura that extend to the middle of the collar (Fig. 2E, G).

Collar. The dorsal mesentery usually starts at the first nerve root and is completed at the end of the collar, although in the holotype the dorsal mesentery was completely absent. The ventral mesentery is completely absent. The anterior neuropore is present (Fig. 2D), but the posterior neuropore may be present or absent. The main lumen of the nerve cord is absent and there are numerous isolated cavities. One to three nerve roots are present. The perihaemal cavities extend to the proboscis pore and are almost entirely separated from each other by the dorsal vessel (Fig. 2D). The collar pores, with thin epithelium and dorsal fold, open to the outside of the body through the first branchial sac.

Trunk. The dorsal mesentery is present in the entire length of the trunk, except for the posterior part of the caudal region (Fig. 2I). The ventral mesentery is present in the entire length of the trunk. At the end of the caudal region, the ventral mesentery is replaced by the pygochord (Fig. 2J). In some specimens, the parabranchial ridges are pronounced. The size of the ventral pharynx is equal to or smaller than that of the dorsal pharynx. There are 15 to 21 synapticles in each tongue bar. The epibranchial ridge is flat and is situated at the same height as the tongue bar (Fig. 2F). The tongue bars protrude more toward the pharynx than do the septa. There is no ventral blind sac among the branchial sacs (Fig. 2F). The first branchial sacs open to the outer side, and all the other sacs open to the medial side, of the genital wings. There is no common gill pore. The postbranchial canal without dorsal blind sac extends straight backward. The lateral septa, connecting to the genital wings at the dorsal side where the primary gonad pores open, extend from the middle of the branchiogenital region to the posterior end of the genital region. The lateral lobes of the gonads reach the edges of the genital wings in the genital region but not in the branchiogenital region. There is no secondary gonad pore. A pair of longitudinal ciliary grooves, located at the dorsolateral sides of the gut, extends from the middle of the genital region to the anterior one-third of the caudal region.

Development

From January to early March, sexually mature individuals of *B. simodensis* can be collected in Kujuppama, Shimoda. In *B. misakiensis*, the color of the gonads can be used to determine the sex of each individual (Urata and Yamaguchi, 2004). Although *B. simodensis* is not sexually dimorphic in gonad coloration, it is easy to distinguish females from males because eggs in the gonads can be seen through the skin. There are three reports on the artificial induction of gamete release, both eggs and sperm, in Enteropneusta, namely, for *Saccoglossus kowalevskii* (Colwin and Colwin, 1962), *Ptychodera flava* (Tagawa *et al*., 1998), and *B. misakiensis* (Urata and Yamaguchi, 2004), and all these reports noted that a shift in seawater temperature induced gamete release. As in these species, a shift in seawater temperature from about 13°C to 8–10°C induced gamete release in *B. simodensis*. However, we could induce gamete release in only about half the adults (19 of 35 adults).

The eggs of *B. simodensis* were about 120 μm in diameter and yellowish cream in color (Fig. 3A). As in *B. misakiensis*, each egg was enclosed in a transparent membrane comprised of two layers. The outer layer was lost

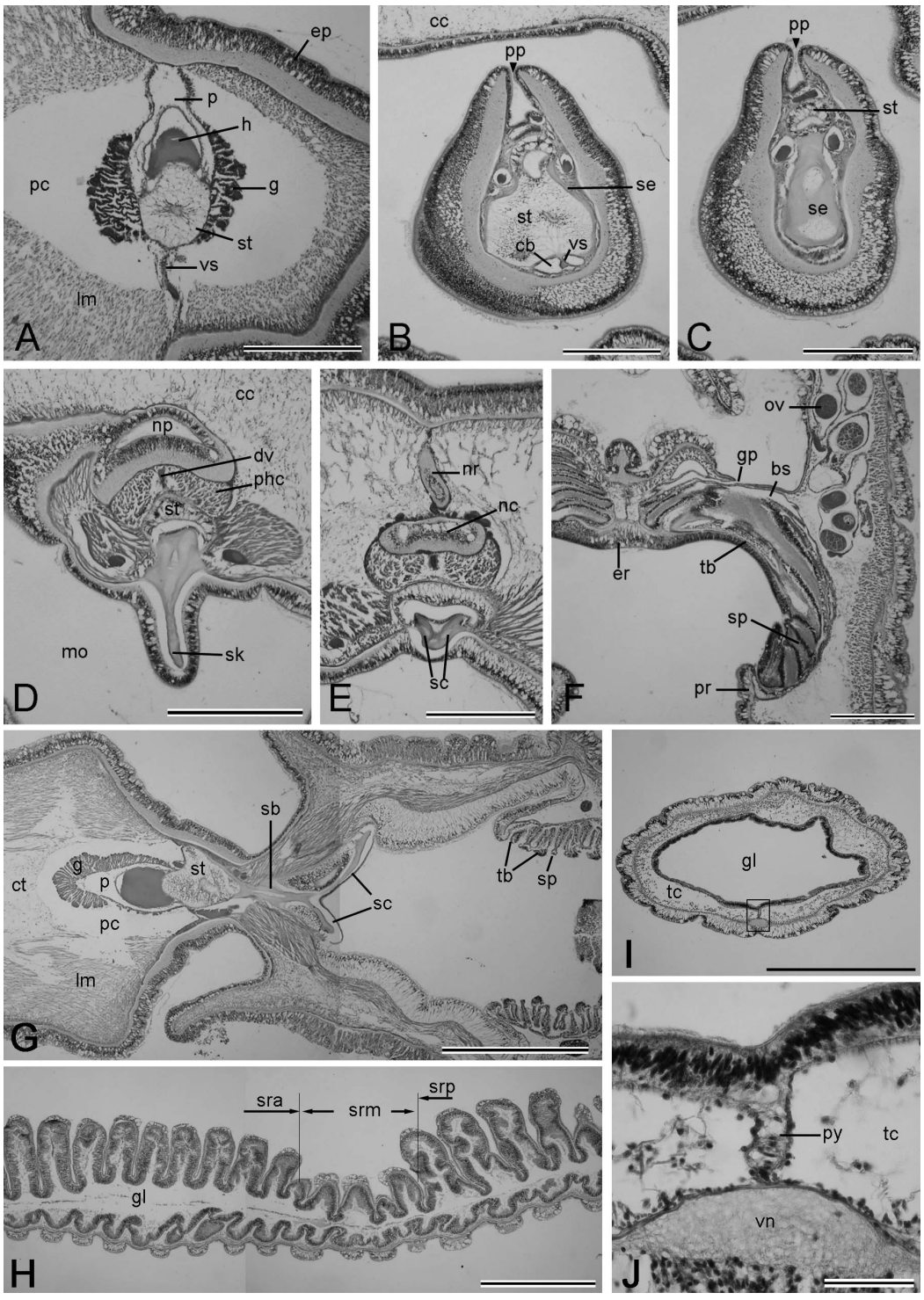

Fig. 2. Sections of *Balanoglossus simodensis*; transverse sections (A–F, I, and J, holotype) with dorsal at top. **(A)** Proboscis organs. **(B)** Proboscis stalk, with the anterior end of the proboscis pore. **(C)** Proboscis stalk, with the posterior end of the proboscis pore. **(D)** Transitional region where the proboscis stalk fuses with the collar. **(E)** Dorsal part of the collar. The proboscis skeleton begins to bifurcate into two crura. **(F)** Branchiogenital region. **(G)** Horizontal section from the middle proboscis (at left) to the anterior end of the trunk. **(H)** Longitudinal section of the hepatic region, with anterior at left and dorsal at top. **(I)** Posterior part of the caudal region. **(J)** High magnification of the boxed area shown in Fig. 2I. **bs**, branchial sac; **cb**, coelomic blind sac; **cc**, collar coelom; **ct**, connective tissue; **dv**, dorsal vessel; **ep**, epidermis; **er**, epibranchial ridge; **g**, glomerulus; **gl**, gut lumen; **gp**, gill pore; **h**, heart; **lm**, longitudinal muscle; **mo**, mouth; **nc**, nerve cord; **np**, neuropore; **nr**, nerve root; **ov**, ovary; **p**, pericardium; **pc**, proboscis coelom; **phc**, perihaemal cavity; **pp**, proboscis pore; **pr**, parabranchial ridge; **py**, pygochord; **sb**, body of the proboscis skeleton; **sc**, crus of the proboscis skeleton; **se**, endplate of the proboscis skeleton; **sk**, keel of the proboscis skeleton; **sp**, septum; **sra**, anterior subregion of the hepatic region; **srm**, middle subregion of the hepatic region; **srp**, posterior subregion of the hepatic region; **st**, stomochord; **tb**, tongue bar; **tc**, trunk coelom; **vn**, ventral nerve cord; **vs**, ventral septum of the proboscis. Scale bars: **A**–**F**=200 μm; **G**–**I**=1 mm; **J**=50 μm.

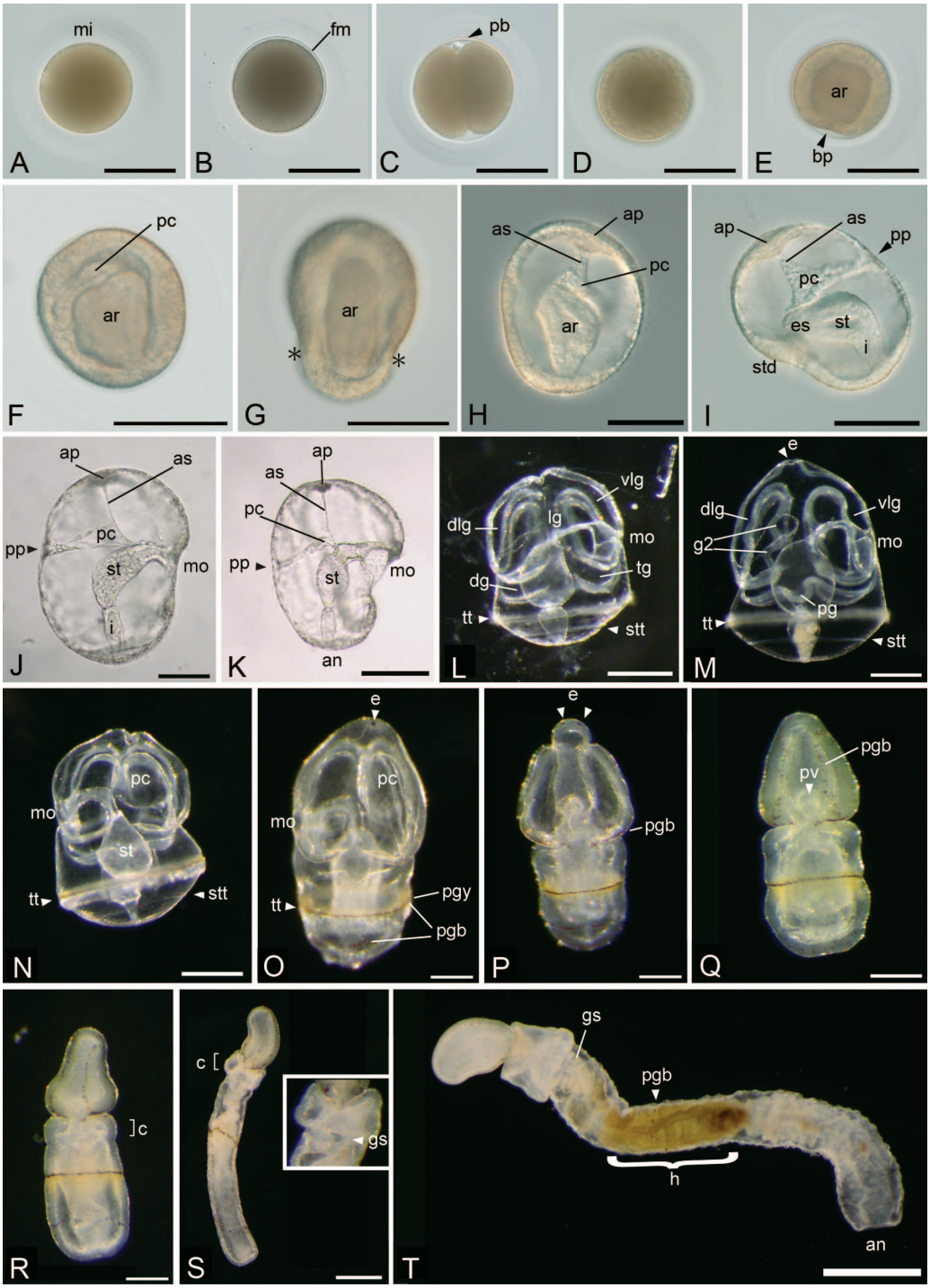

Fig. 3. Development of *Balanoglossus simodensis* from unfertilized egg to juvenile. **(A)** Unfertilized egg. **(B)** Fertilized egg. **(C)** Two-cell-stage embryo, 3 hr after insemination. **(D)** Blastula, 18 hr after insemination. **(E)** Lateral view of mid gastrula, 32 hr after insemination. **(F)** Right lateral view of 39-hr-old gastrula. **(G)** Larva extruding from the fertilization membrane, 48 hr after insemination. Asterisks indicate the opening in the fertilization membrane. **(H)** Left lateral view of an embryo just after hatching. **(I)** Left lateral view of a larva 8 hr after hatching. **(J)** Right lateral view of a Müller-stage larva 1 day after hatching. **(K)** Right lateral view of a Heider-stage larva 2 days after hatching. **(L)** Right lateral view of a Metschnikoff-stage larva 20 days after hatching. **(M)** Right lateral view of a Krohn-stage larva 1 month after hatching. **(N)** Left lateral view of a Spengel-stage larva 2 months after hatching. **(O)** Left lateral view of a juvenile 5 hr after settlement. **(P)** Dorsal view of a juvenile 11 hr after settlement. **(Q)** Dorsal view of a juvenile 1 day after settlement. **(R)** Dorsal view of a juvenile 2 days after settlement. **(S)** Dorsal view of a juvenile 5 days after settlement. **(T)** Dorsal view of a juvenile 1 month after settlement. **an**, anus; **ap**, apical plate; **ar**, archenteron; **as**, apical strand; **bp**, blastopore; **c**, collar; **dg**, dorsal groove; **dlg**, dorsolateral groove; **e**, eye; **es**, esophagus; **fm**, fertilization membrane; **g2**, secondary groove; **gs**, gill slit; **h**, hepatic region; **i**, intestine; **lg**, lateral groove; **mi**, inner layer of egg membrane; **mo**, mouth; **pb**, polar body; **pc**, protocoel; **pg**, posterior groove; **pgb**, brown pigmented cells; **pgy**, yellow pigmented cells; **pp**, proboscis pore; **pv**, proboscis vesicle; **st**, stomach; **std**, stomodeum; **stt**, secondary telotroch; **tg**, transverse groove; **tt**, telotroch; **vlg**, ventrolateral groove. Scale bars: **A**–**J**=100 μm; **K**, **O**–**R**=200 μm; **L**–**N**, **S**=400 μm; **T**=1 mm.

before spawning. After artificial insemination, the fertilization membrane was elevated very slightly from the egg surface (Fig. 3B). The percentage of the fertilization was low, about 20%. Development was not synchronized in each batch, but occurred similarly among batches. The time course of *B. simodensis* development is presented in Table 1. This table shows the time that we first observed an embryo in each stage. Early embryogenesis from egg to gastrula occurs in a fashion similar to that in *P. flava* (Tagawa *et al.,* 1998). The first cleavage was observed 3 hr after insemination (Fig. 3C). Subsequent cleavages occurred at 1-hr intervals, and 13 hr after insemination the embryo developed into a blastula (Fig. 3D). About 21 hr after insemination, the blastopore formed and the embryo developed into a gastrula (Fig. 3E). Embryos hatched about 48 hr after insemination, at the late gastrula stage (Fig. 3F). Because the embryo was compressed by the fertilization membrane, it did not move within the membrane. The embryo broke the membrane at the posterior side and squeezed through a small hole in the membrane (Fig. 3G). The embryo was covered with cilia, including the long apical tuft, and the part of the body protruding from the fertilization membrane increased in size (Fig. 3H). About 8 hr after hatching, the archenteron of the larva began to differentiate into three sections: esophagus, stomach, and intestine. The mouth and anus were still closed (Fig. 3I). One day after hatching, the larva developed the longitudinal ciliary band but not the telotroch; that is, it was in the Müller stage, in which both the mouth and anus are open (Fig. 3J). The telotroch became noticeable 2 days after hatching, and this was characteristic of the Heider stage (Fig. 3K). The larva gradually developed a primary lobe and saddle, increased in size, and reached the Metschnikoff stage (Fig. 3L). The secondary telotroch was evident by this stage. Subsequently, about 1 month after hatching, the larva developed a secondary lobe and saddle, which were characteristic of the Krohn stage (Fig. 3M).

Table 1. Timetable of Development of *Balanoglossus simodensis* at 17–20°C

Developmental stages	Time (hr) after insemination
1st polar body formation	0.8
2nd polar body formation	1.3
2-cell stage	3.0
4-cell stage	4.0
8-cell stage	5.0
16-cell stage	6.0
32-cell stage	7.0
Blastula	13.0
Gastrula	21.0
Hatching	48.0

After 2 months of floating as plankton, the larva decreased in size, the protocoel increased in size, and the secondary lobe and saddle began to degenerate; thus, it became a Spengel-stage larva (Fig. 3N). Two types of pigmented cells, brown and yellow, appeared in the telotroch but not in the secondary telotroch. In this stage, the larva began to move to the bottom of the glass beaker if the water remained still (i.e., without stirring), and began metamorphosis if grains of sand were laid on the glass beaker's bottom. After settlement, the larva did not elongate, but it decreased in width; as a result, its body became cylindrical. Only brown-pigmented cells appeared in the secondary telotroch and longitudinal ciliary band (Fig. 3O). The telotroch disappeared by 11 hr after settlement (Fig. 3P). One day after settlement, the proboscis was evident, but the boundary between the collar and trunk was not distinct (Fig. 3Q). The juvenile secreted mucus and burrowed in the sand using its proboscis. By 2 days after settlement, the boundary between the collar and trunk became clear except on the dorsal side of the collar (Fig. 3R). The first gill pore formed by 5 days after settlement, and the dorsal side of the collar had already formed (Fig. 3S). The hepatic region formed in the vicinity of the brown pigmented cells where the telotroch had been (Fig. 3T).

DISCUSSION

Balanoglossus simodensis is easily distinguished from previously reported species by the hepatic region with three distinct subregions. No other species has the middle subregion with tiny or no hepatic saccules. *Balanoglossus australiensis* (Hill, 1894) and *Balanoglossus capensis* (Gilchrist, 1908; Horst, 1937) are morphologically similar to *B. simodensis*. In these two species, however, the saccules gradually increase in size from the anterior to the middle part of the hepatic region, remain large in the middle part, and then gradually decrease in size toward the posterior part. Although *B. stephensoni* (Horst, 1937) is also morphologically similar to *B. simodensis*, the former does not have the middle subregion of the hepatic region, which in contrast to *B. simodensis* begins and ends abruptly. We observed several specimens of other balanoglossids: *B. carnosus*, *B. misakiensis*, and an unidentified species. In *B. carnosus,* there is no transitional zone between the genital region and the hepatic region. The hepatic saccules form a regular row on each side. The anterior saccules are large and gradually decrease in size. The saccules are very wide and flat. In *B. misakiensis,* there is a transitional zone between the genital region and the hepatic region, and the hepatic saccules form a regular row on each side. The saccules gradually increase in size, maintain their size in middle part, and then gradually decrease in size. In an undescribed balanoglossid collected in Sagami Bay, there is a transitional zone between the genital region and the hepatic region. The hepatic saccules form a regular row on each side, and the anterior and posterior ends of the hepatic region are distinct. The hepatic region is divided into two distinct subregions, an anterior one with small saccules and a posterior one with large saccules.

The morphology and arrangement of saccules in the hepatic region of balanoglossids are species-specific characters and are well conserved within species. For this reason, the appearance of the hepatic region is one of the most useful characters for identification. Although, internal features have been well described for the identification of enteropneust species, there is no specific internal feature that is useful to identify *B. simodensis*. In this species, we observed considerable variation in some internal features, such as the branching pattern of the lumen of the stomochord, the number of nerve roots, presence or absence of

neuropores, and the number of synapticles. We believe that internal features should be reevaluated by detailed observation of many specimens of each species.

We were able to induce gamete release in *B. simodensis*; however, the success rate was not high. The success rate of the fertilization was also low, and the development of embryos was not synchronized. These results may have been due to the method of induction of oocyte maturation, and sperm activation may not have been complete. Although we observed the development of *B. simodensis* in this study, improvement of the method of artificial fertilization remains an important problem.

The morphology of the tornaria larva seems to correlate closely with the length of the larval period. The morphogenesis of the tornaria larva is divided into two phases, the progressive and regressive phases. In the progressive phase, the larva increases in size and develops the longitudinal ciliary band. In the regressive phase, the larva decreases in size and the longitudinal ciliary band degenerates. After this phase, the larva metamorphoses into the adult form. The progressive development of *B. simodensis* resembles that of *B. clavigerus*, which passes through the Müller, Heider, Metschnikoff, and Krohn stages (Colwin and Colwin, 1988). *Balanoglossus misakiensis* has a short larval period, about a week, and lacks the Krohn stage (Urata and Yamaguchi, 2004). The larval period of *B. simodnesis* and *B. clavigerus* is about 2 months, and both species have Krohn-stage larvae with a simple secondary lobe and saddle. *Ptychodera flava* has a very long larval period, longer than 6 months, and its Krohn-stage larva develops the secondary lobe and saddle into tentacles (Hadfield, 1975). In short, the longer the larval period, the more complex the larval morphology becomes.

Hemichordates have been rather poorly investigated, despite their interesting phylogenetic position. Recently, Lowe *et al.* (2003, 2006) examined the direct-developing enteropneust *Saccoglossus kowalevskii*; the embryogenesis of the indirect-developing enteropneust *P. flava* (Tagawa *et al.*, 2001; Nakajima *et al.*, 2004) has been well examined. These studies provided new insights into the evolution of deuterostomes. Nevertheless, the long larval period of *P. flava* (longer than 6 months) has made it difficult to study its metamorphosis. *Balanoglossus misakiensis* has a short larval period (about a week) and is thus very useful for studying metamorphosis (Urata and Yamaguchi, 2004). However, as individuals of *B. misakiensis* are relatively large (longer than 20 cm) and live in the subtidal zone, it is difficult to collect them without damage. It is also difficult to rear these worms in the laboratory. In contrast, *B. simodensis* is one of the shortest enteropneusts (up to 10 cm), and it inhabits the intertidal zone. It is therefore easy to collect many intact worms, and furthermore it is relatively easy to keep them in the laboratory. We also succeeded in both rearing planktonic larvae to juveniles and observing metamorphosis in *B. simodensis*, despite its relatively long larval period (2 months). In the future, we will establish an inland culture system for *B. simodensis*, making it a useful model animal not only for developmental biology but also for other biological fields such as genetics.

There is very little taxonomical and ecological information about enteropneusts. To examine their morphology and behavior, intact worms are necessary. As mentioned above, it is very difficult to collect intact worms from the subtidal zone. If worms are collected by a dredge or Ekman grab, almost all are damaged, and we cannot learn about their habitats. For this reason, many of the enteropneusts previously described were from restricted habitats of the intertidal zone. We recently performed careful sampling and observation of their habitats by scuba diving in the subtidal zone, from 3 to 15 m in depth, and have collected five apparently undescribed species from the Izu Peninsula. Thus careful sampling by scuba diving in the subtidal zone will provide much information on the taxonomy and ecology of enteropneusts, even though the depth of the water restricts sampling.

ACKNOWLEDGMENTS

We thank Professor Teruaki Nishikawa (Nagoya University Museum) for allowing us to refer to some articles and for his encouragement. We also thank the staff of Shimoda Marine Research Center (University of Tsukuba) for their kind assistance and hospitality during this work. This study is contribution No. 733 from Shimoda Marine Research Center.

REFERENCES

Benito J, Pardos F (1997) Hemichordata. In “Microscopic Anatomy of the Invertebrates Vol 15” Ed by FW Harrison, EE Ruppert, Wiley-Liss, New York, pp 15–101

Colwin AL, Colwin LH (1988) Hemichordata. In “Development of Invertebrates Vol 2” Ed by K Dan, K Sekiguchi, H Ando, H Watanabe, Baifukan, Tokyo, pp 411–429 (in Japanese)

Colwin LH, Colwin AL (1962) Induction of spawning in *Saccoglossus kowalevskii* (Enteropneusta) at Woods Hole. Biol Bull 123: 493

Gilchrist JDF (1908) New forms of the Hemichordata from South Africa. Trans South Africa Philos Soc 17: 151–176

Hadfield MG (1975) Hemichordata. In “Reproduction of Marine Invertebrates Vol 2” Ed by AC Giese, JS Pearse, Academic Press, New York, pp 185–240

Hill JP (1894) On a new species of Enteropneusta (*Ptychodera australiensis*) from the coast of New South Wales. Proc Linn Soc NSW 10: 1–42

Holland ND, Clague DA, Gordon DP, Gebruk A, Pawson DL, Vecchione M (2005) ‘Lophoenteropneust’ hypothesis refuted by collection and photos of new deep-sea hemichordates. Nature 434: 374–376

Horst CJ van der (1937) On a new South African species of *Balanoglossus* and a comparison between it and *Balanoglossus capensis* (Gilchrist). Ann South Africa Mus 32: 69–93

Horst CJ van der (1939) Hemichordata. In “Klassen und Ordnungen des Tierreiches Vol 4” Ed by HG Broon, Akademische Verlagsgesellschaft, Leipzig, pp 1–737

Horst CJ van der (1940) The Enteropneusta from Inyack Island, Delagoa Bay. Ann South Africa Mus 32: 293–380

Lowe CJ, Wu M, Salic A, Evans L, Lander E, Stange-Thomann N, Gruber CE, Gerhart J, Kirschner M (2003) Anteroposterior patterning in hemichordates and origins of the chordate nervous system. Cell 113: 853–865

Lowe CJ *et al.* (2006) Dorsoventral patterning in hemichordates: insight into early chordate evolution. PLoS Biol 4: 1603–1619

Nakajima Y, Humphreys T, Kaneko H, Tagawa K (2004) Development and neural organization of the tornaria larva of the Hawaiian hemichordate, *Ptychodera flava*. Zool Sci 21: 69–78

Nishikawa T (1977) Preliminary report on the biology of the enteropneust, *Ptychodera flava* ESCHSCHOLTZ, in the vicinity of Kushimoto, Japan. Publ Seto Mar Biol Lab 23: 393–419

Stiasny G (1929) Tornaria von Japan. Zool Jahrb Abt Syst 56: 67–

92
Stiasny-Wijnhoff G, Stiasny G (1927) Die Tornarien. Ergebn Fortschr Zool 7: 38–208
Tagawa K, Nishino A, Humphreys T, Satoh N (1998) The spawning and early development of the Hawaiian acorn worm (hemichordate), *Ptychodera flava*. Zool Sci 15: 85–91
Tagawa K, Satoh N, Humphreys T (2001) Molecular studies of hemichordate development: a key to understanding the evolution of bilateral animals and chordates. Evo Dev 3: 443–454
Tokioka T (1937) *Tornaria susakiensis* n. sp., a new tentaculated tornaria-larva. Annot Zool Japan 16: 341–344
Urata M, Yamaguchi M (2004) The development of the enteropneust hemichordate *Balanoglossus misakiensis* KUWANO. Zool Sci 21: 533–540
Woodwick KH, Sensenbaugh T (1985) *Saxipendium coronatum*, new genus, new species (Hemichordata: Enteropneusta): the unusual spaghetti worms of the Galápagos Rift hydrothermal vents. Proc Biol Soc Wash 98: 351–365

(Received February 16, 2007 / Accepted August 1, 2007)